On the Concept of the Multi-Source Inverter for Hybrid Electric Vehicle Powertrains

Lea Dorn-Gomba, *Student Member, IEEE*, Pierre Magne, *Member, IEEE*, Benjamin Danen, and Ali Emadi, *Fellow, IEEE*

***Abstract*—This paper presents an inverter topology named the multi-source inverter that aims to connect several independent DC sources to the same AC output using a single stage of conversion. This power converter has been developed for applications, such as electrified powertrains. Compared to the conventional hybrid powertrains that use a DC/DC converter to provide an adaptable voltage to the load, the multi-source inverter can drive a traction motor from variable DC voltages without the use of an additional power converter. Hence, the high power DC/DC converter can be dissociated from the traction mode and its use will be restricted to the engine's start-up and regenerative braking, allowing a significant reduction of its power rating from tens of kWatts to a few kWatts. The overall efficiency of the electrified traction drive can also be improved due to the single conversion stage between the battery and the motor. In this paper, the multi-source inverter topology is introduced and its different operating modes are determined through the study of the inverter circuit. Closed-loop control simulations and experiments with a scaled-down prototype and an induction motor were performed to validate the effectiveness of the proposed topology and concept.**

***Index Terms*—Inverters, power electronics, pulse width modulated inverters, traction motor drives, transportation.**

I. Introduction

MOTIVATED by the need to significantly reduce fuel consumption and harmful emissions in transportation, the interest for electrified powertrains keeps growing in the automotive industry. Electric vehicles (EVs), hybrid electric vehicles (HEVs), and plug-in HEVs (PHEVs) currently achieve promising performances in comparison to the internal combustion engine (ICE) vehicles [1]–[4]. Although EVs are a very good candidate to overcome the current environmental issues associated with transportation, they possess drawbacks including the energy-storage limitations of their battery. On the other hand, HEVs and PHEVs have improved the vehicle performance thanks to the combination of one or two electric machines (EMs) with the ICE. In a power-split architecture (such as in the Toyota Prius), two electric machines are mechanically coupled with the ICE through a planetary gear system and can operate either as motor or generator. This combination of power sources allows for different operating modes at high efficiency [5]. Moreover, a smaller battery pack can be used compared to the one integrated in EVs allowing volume and cost reductions. Indeed, EVs have a larger battery pack than HEVs and PHEVs due to the fact that they only have one source of energy to power the wheels. For instance, the Tesla Model S 2014 has a battery pack of 85 kWh while the HEV Toyota Prius 2010 and the Toyota PHEV 2013 have a battery pack of 1.3 and 4.4 kWh, respectively [6].

Power electronic circuits connect the battery pack to the EMs and are composed of various components with numerous interactions between them. Therefore, even if combining electrical and combustion engines reduces the volume and the cost of the battery pack, it also increases the overall complexity of the system. Power converters and electric machines used in these traction drive systems play a major role since they enable higher efficiency and, hence, fuel consumption reductions compared to ICE vehicles [7], [8]. They have been in the spotlight for the past few years and intensive research attempts to reach the targets defined by the U.S. Department of Energy for 2020 [9]–[11]. Low cost, high efficiency, and high power density are the three main challenges for these components to meet.

In a simple electrified powertrain architecture, the traction inverter directly connects the battery pack to the electrical machine without the use of any additional power converters [12], [13]. Although this configuration is less costly and less complex regarding the control of the power electronic systems, it also achieves reduced efficiency at light load due to the use of a fixed DC-link voltage. One solution widely applied in most of the recent HEVs and PHEVs consists of using a DC–DC boost converter between the battery and the DC-link of the traction inverters [see Fig. 1(a)] [5], [14]–[16]. By doing so, the voltage of the battery is stepped up accordingly to the driving conditions in order to ensure the operation of the inverter and the traction motor at high efficiency [17]–[20]. This architecture presents several additional advantages, such as extending the constant torque characteristic, reducing the current rating on the switches, and having a higher inverter power supply voltage without increasing the battery voltage. However, a high power DC/DC converter also has some demerits since its power rating must match that of the battery pack in order to avoid derating the battery system. Indeed, as the battery and the DC/DC converter are

Manuscript received May 31, 2017; revised August 27, 2017; accepted October 10, 2017. Date of publication October 22, 2017; date of current version June 22, 2018. This research was supported by the Canada Excellence Research Chairs Program. Recommended for publication by Associate Editor G. Oriti. *(Corresponding author: Lea Dorn-Gomba.)*

L. Dorn-Gomba, B. Danen, and A. Emadi are with the McMaster Institute for Automotive Research and Technology, McMaster University, Hamilton, ON L8S 4L8, Canada (e-mail: dorngoml@mcmaster.ca; danenbh@mcmaster.ca; emadi@mcmaster.ca).

P. Magne is with the APOJEE, Clermont-Ferrand 63100, France (e-mail: pierre.magne@apojee.eu).

Color versions of one or more of the figures in this paper are available online at http://ieeexplore.ieee.org.

Digital Object Identifier 10.1109/TPEL.2017.2765247

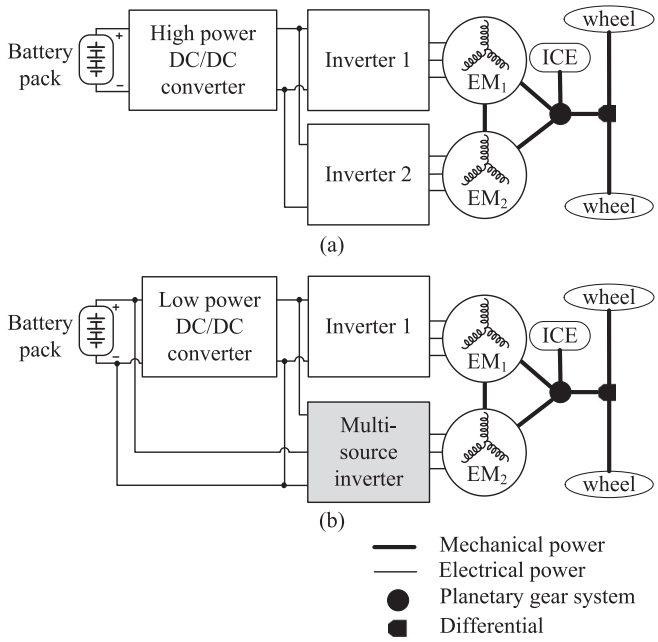

Fig. 1. (a) Conventional hybrid powertrain such as in the Toyota Prius. (b) Suggested hybrid powertrain with the multi-source inverter.

in series, the power rating of the two is limited by the lowest one. As a result, a high power battery pack and, hence, a high power DC/DC converter, will adversely impact on the power density and cost of the powertrain due to the inductor, which is usually bulky and expensive. Furthermore, as this requires the addition of a conversion stage, it directly affects the overall efficiency of the powertrain system during both traction and regenerative braking mode.

Traction inverters draw attention to improve the performance of the electrified propulsion system since they are the essential components ensuring the power conversion from the battery to the electric machines [21]. Traditional two-level inverters are extensively used in the electrified transportation industry due to their low cost and simple control. However, with the continuous increase of the power requirements, this topology shows some limitations because of its high switch power rating and high power losses. Indeed, the voltage across each switch is equal to the DC-link voltage and high blocking voltage switches tend to have higher switching loss. Moreover, for high current rating applications, several devices need to be used in parallel which increases the conduction losses and reduces the power density of the converter. On the other hand, multilevel inverters have been developed specifically for high-voltage applications since the blocking voltage of some switches can be considerably reduced [22]–[26]. They also offer other advantages such as low total harmonic distortion (THD) and low power losses compared to two-level inverters. Nevertheless, the complexity of their control and their cost still restrain their use in traction drive systems. Numerous innovative inverter topologies for high-voltage applications have been suggested in the literature [27]–[34]. Among them, the Z-source inverter furthers its reputation for electrical propulsion systems since it also offers an adjustable stepped up voltage to the load without the use of a DC/DC converter.

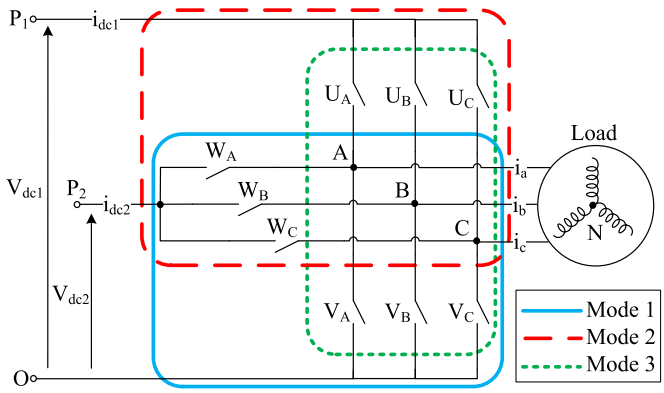

Fig. 2. Multi-source inverter topology with two DC inputs.

However, its competitiveness is adversely affected by its high switch rating and large volume of the passive components for a similar efficiency compared to a two-level inverter combined with a DC/DC boost converter [35], [36].

This paper presents an inverter topology named the multi-source inverter [37], [38]. Its fundamental purpose is to connect distinct DC sources to the same AC output using a single conversion stage. When applied to HEV and PHEV powertrains, the input of this topology is directly connected to the battery pack and the high DC-link voltage shared with the other inverter [see Fig. 1(b)]. As a result, the battery pack can immediately transfer power to the traction motor without stepping up its voltage with a DC/DC converter. Moreover, this high power DC/DC converter can be dissociated from the traction mode and only used to start the ICE and in regenerative braking. Indeed, unlike in conventional hybrid powertrains, the battery and the DC/DC converter are not connected in series anymore but in parallel. Hence, the DC/DC converter can be bypassed in traction mode and a significant reduction of its power rating from tens of kWatts to a few kWatts can be achieved without derating the battery system. Moreover, the overall efficiency of the electrified traction drive can be improved due to the single conversion stage between the battery and the motor.

In the following sections, the operating modes and the control strategy of the multi-source inverter are first presented. Then, a comprehensive analysis of the benefits of this power converter applied to hybrid powertrain systems is discussed. Finally, closed-loop control simulations and experiments with an induction motor verify and validate the concept of the proposed topology.

II. Multi-source Inverter

The multi-source inverter is a power converter which aims to connect several DC sources to the same AC output using a single stage of conversion. For instance, Fig. 2 shows the topology with two DC inputs connected between (O) and (P_1) and (O) and (P_2). When the multi-source inverter is applied to hybrid powertrains, the DC-link voltage V_{dc1} is shared with the other inverter while V_{dc2} is supplied by a battery pack.

By replacing the ideal switches $U_{A,B,C}$, $V_{A,B,C}$, and $W_{A,B,C}$ in Fig. 2 by Insulated Gate Bipolar Transistors (IGBTs), two pos-

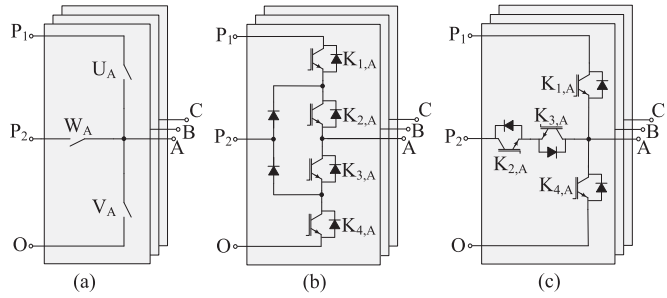

Fig. 3. Multi-Source inverter topology with (a) Ideal switches. (b) NPC-based circuit. (c) T-NPC-based circuit.

sible circuits can be used to model the multi-source inverter and are very similar to three-level inverters, namely the Neutral Point Clamped (NPC) and T-NPC topologies (see Fig. 3). However, unlike these conventional three-level inverters, the multi-source inverter does not have a neutral point connecting the upper and lower switches of each leg. This means that each input capacitor voltage in the proposed topologies is equal to the source voltage respectively across, instead of one-half of the DC input voltage, as it is the case for three-level inverters. As a result, the input sources of the multi-source inverter are completely independent.

A. Operating Modes

Regarding to the state of the switches, it can be seen that the multi-source inverter is composed of three standard two-level inverters (see Fig. 2). Hence, three different input voltages can be applied to the output line-to-line voltages, implying three distinct operating modes:

- *Mode 1:* Only the battery ($V_{\mathrm{dc}2}$) supplies the motor by using the switches $W_{A,B,C}$ and $V_{A,B,C}$.
- *Mode 2:* The high DC-link voltage ($V_{\mathrm{dc}1}$) supplies the motor while charging the battery ($V_{\mathrm{dc}2}$). The switches $U_{A,B,C}$ and $W_{A,B,C}$ are used and the voltage applied to the output is equal to $V_{\mathrm{dc}1}$-$V_{\mathrm{dc}2}$.
- *Mode 3:* Only the high DC-link ($V_{\mathrm{dc}1}$) voltage supplies the motor by using the switches $U_{A,B,C}$ and $V_{A,B,C}$.

The line-to-line voltages $[V_{AB}, V_{BC}, V_{CA}]$ and phase voltages $[V_{AN}, V_{BN}, V_{CN}]$ are calculated with the well-known formulas:

$$\begin{aligned} V_{AB} &= V_{AN} - V_{BN} \\ V_{BC} &= V_{BN} - V_{CN} \\ V_{CA} &= V_{CN} - V_{AN} \end{aligned} \tag{1}$$

$$\begin{bmatrix} V_{AN} \\ V_{BN} \\ V_{CN} \end{bmatrix} = \frac{1}{3} \begin{bmatrix} 2 & -1 & -1 \\ -1 & 2 & -1 \\ -1 & -1 & 2 \end{bmatrix} \times \begin{bmatrix} V_{AO} \\ V_{BO} \\ V_{CO} \end{bmatrix} \tag{2}$$

According to Fig. 3(b) and (c), the voltages $[V_{AO}, V_{BO}, V_{CO}]$ in both NPC-based and T-NPC-based circuits can be expressed as functions of the gate signal of the switches and the DC-bus voltages:

$$\begin{aligned} V_{AO} &= F_A V_{\mathrm{dc}1} + G_A V_{\mathrm{dc}2} - Z_A.i_A \\ V_{BO} &= F_B V_{\mathrm{dc}1} + G_B V_{\mathrm{dc}2} - Z_B.i_B \\ V_{CO} &= F_C V_{\mathrm{dc}1} + G_C V_{\mathrm{dc}2} - Z_B.i_C \end{aligned} \tag{3}$$

where Z_i is the phase impedance of the load, $i = A, B,$ or C is the corresponding phase, $F_i = K_{1,i}.K_{2,i}$ with "." the AND sign in Boolean logic and $G_i = K_{1,i} \oplus K_{2,i}$ with "$\oplus$" the XOR sign in Boolean logic.

Hence, the combination of the two DC sources enables supplying the load with seven different line-to-line voltages according to the state of the switches. Table I summarizes the switching combinations with the ideal switches and neglects the voltages produced by the impedance Z_i in each phase shown in (3).

Moreover, considering a Y connection of the load (three phases AC motor), the DC-side current equations $[i_{\mathrm{dc}1}, i_{\mathrm{dc}2}]$ are given by:

$$\begin{aligned} i_{\mathrm{dc}1} &= F_A i_A + F_B i_B + F_C i_C \\ i_{\mathrm{dc}2} &= G_A i_A + G_B i_B + G_C i_C \end{aligned} \tag{4}$$

From the above mentioned equations, it can be seen that the three operating modes of the multi-source inverter enable different voltages to supply the motor. Therefore, the battery pack can be used to start the motor and for low speeds while the high DC bus can provide power for middle and high speeds, as it is traditionally done with a conventional traction inverter. However, compared to typical hybrid powertrains, the multi-source inverter provides an adaptable voltage with the additional benefit of not using a DC/DC boost converter. This results in simplifying the control of the power converters and improving the overall efficiency of the traction drive system. The DC/DC boost converter will only be used to start the ICE and charge the battery with regenerative braking. Hence, its power rating is not related to the battery pack power and can be derated to save cost and volume. The benefits of the multi-source inverter will be further discussed in Section III.

B. Adapted Pulse Width Modulation Strategy

Space Vector Pulse Width Modulation (SVPWM) is usually preferred in automotive motor drive applications because it offers better controllability at high speed in comparison to the sinusoidal PWM. Also, it presents better performance in term of THD in control of AC motor and DC bus utilization [39]–[41]. As previously mentioned, the multi-source inverter topology is very similar to NPC and T-NPC inverter circuits. Thus, an adapted SVPWM strategy was developed to control the switches in the multi-source inverter based on its similarities with these three-level inverters.

As the widely used SVPWM, the new strategy consists of applying the reference voltage by a combination of the two nearest vectors and one zero vector in the alpha-beta reference plane [42]. The main difference between the adapted SVPWM and the typical one is related to the switching states. For three-level inverters, three switching states -1, 0, and 1 represent the three phase voltage status of each leg (respectively $-V_{\mathrm{dc}}/2$, 0, $V_{\mathrm{dc}}/2$) [see Fig. 4(a)] . However, since the DC source voltage can

TABLE I
SWITCHING COMBINATIONS OF THE MULTI-SOURCE INVERTER

Modes	States of switches									Line-to-line voltages		
	U_1	U_2	U_3	V_1	V_2	V_3	W_1	W_2	W_3	V_{AB}	V_{BC}	V_{CA}
1	Always open			0	1	1	1	0	0	V_{dc2}	0	$-V_{dc2}$
				0	0	1	1	1	0	0	V_{dc2}	$-V_{dc2}$
				1	0	1	0	1	0	$-V_{dc2}$	V_{dc2}	0
				1	0	0	0	1	1	$-V_{dc2}$	0	V_{dc2}
				1	1	0	0	0	1	0	$-V_{dc2}$	V_{dc2}
				0	1	0	1	0	1	V_{dc2}	$-V_{dc2}$	0
2	1	0	0	Always open			0	1	1	$V_{dc1}-V_{dc2}$	0	$-(V_{dc1}-V_{dc2})$
	1	1	0				0	0	1	0	$V_{dc1}-V_{dc2}$	$-(V_{dc1}-V_{dc2})$
	0	1	0				1	0	1	$-(V_{dc1}-V_{dc2})$	$V_{dc1}-V_{dc2}$	0
	0	1	1				1	0	0	$-(V_{dc1}-V_{dc2})$	0	$V_{dc1}-V_{dc2}$
	0	0	1				1	1	0	0	$-(V_{dc1}-V_{dc2})$	$V_{dc1}-V_{dc2}$
	1	0	1				0	1	0	$V_{dc1}-V_{dc2}$	$-(V_{dc1}-V_{dc2})$	0
3	1	0	0	0	1	1	Always open			V_{dc1}	0	$-V_{dc1}$
	1	1	0	0	0	1				0	V_{dc1}	$-V_{dc1}$
	0	1	0	1	0	1				$-V_{dc1}$	V_{dc1}	0
	0	1	1	1	0	0				$-V_{dc1}$	0	V_{dc1}
	0	0	1	1	1	0				0	$-V_{dc1}$	V_{dc1}
	1	0	1	0	1	0				V_{dc1}	$-V_{dc1}$	0

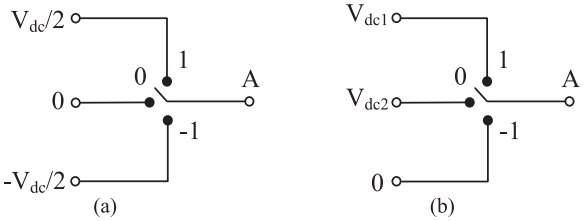

Fig. 4. (a) Switching states in a three-level inverter. (b) In the multi-source inverter.

be equal to either $V_{\rm dc1}$ or $V_{\rm dc2}$ in the multi-source inverter, each operating mode is reachable by only two of the three switching states in each leg [see Fig. 4(b)].

Table II summarizes the device switching states in each operating mode of the multi-source inverter for both TNPC and NPC-based circuits shown in Fig. 3(b) and (c). It should be also noted that the devices $K_{3,i}$ and $K_{4,i}$ are the complementary of $K_{1,i}$ and $K_{2,i}$ respectively.

From Table II, it can be seen that Mode 1 is reachable by the switching states 0 and -1 which means that for each leg $K_{1,i}$ stays switched off, $K_{3,i}$ stays switched on and only $K_{2,i}$ and $K_{4,i}$ are switching. If the multi-source inverter is in Mode 2, the switching states are 0 and 1, where $K_{2,i}$ stays switched on, $K_{4,i}$ stays switched off and only $K_{1,i}$ and $K_{3,i}$ are switching. Finally, Mode 3 is reachable when the switching states are 1 and -1, implying the switching of $K_{1,i}$, $K_{2,i}$, $K_{3,i}$, and $K_{4,i}$.

The spatial representation in alpha-beta diagram of the new SVPWM strategy is composed of three hexagons, whose size varies depending on the voltage applied to the load (see Fig. 5). Indeed, the radius of the inner circle of each hexagon represents the maximum voltage $V_{\rm lim1}$, $V_{\rm lim2}$, or $V_{\rm lim3}$ achievable in Mode 1, 2, or 3 and is equal to $V_{\rm dc2}/\sqrt{3}$, $(V_{\rm dc1}-V_{\rm dc2})/\sqrt{3}$ or $V_{\rm dc1}/\sqrt{3}$, respectively. Each hexagon is composed of six sectors. Compared to the control for a NPC converter, only 21 vectors are used instead of 27 vectors and no region selection is needed, hence, simplifying the control of the inverter. After the mode and sector identification, the switching duration of each vector is calculated such as in a typical SVPWM control scheme. Finally, symmetric switching sequences were chosen here in order to reduce the THD and the number of switching, allowing power loss reductions.

III. BENEFITS OF THE MULTI-SOURCE INVERTER IN HYBRID POWERTRAINS

Most of the recent hybrid architectures, such as the Toyota Prius, use a DC/DC boost converter between the battery pack and the traction inverter to step up the battery voltage regarding the driving requirements. One of the major benefits of this adaptable voltage is to enlarge the high efficiency areas of the inverters and the traction motor [5]. However by considering the complete traction drive system, this DC/DC converter adds a power stage conversion which reduces the overall efficiency and increases the cost and volume. The multi-source inverter has been developed to keep the advantages of supplying the load with distinct voltages while using a single power stage conversion. Indeed, it can be shown that the DC/DC boost converter is bypassed for most of the driving conditions and will be only used to start the ICE and in regenerative braking. On the contrary, in conventional hybrid powertrains composed of a DC/DC converter, the battery voltage will be always stepped up even if its voltage is theoretically sufficient to drive the motor.

The control strategies of electrified powertrains are subject to continuous improvements to ensure the operating of the system at its best performance. These complex techniques are multi-objective functions that aim to achieve numerous goals, such as driving performance optimization, fuel consumption reductions, and gas emission minimization [43]–[45]. In conventional hybrid powertrains, the control of the DC/DC boost converter is based on the vehicle speed but is also influenced by other fac-

TABLE II
DEVICE SWITCHING STATES OF THE MULTI-SOURCE INVERTER

Operating modes of the multi-source inverter	Switching states	Device switching states			
		$K_{1,i}$	$K_{2,i}$	$K_{3,i}$	$K_{4,i}$
1	-1 and 0	OFF	OFF or ON	ON	ON or OFF
2	0 and 1	OFF or ON	ON	ON or OFF	OFF
3	-1 and 1	OFF or ON	OFF or ON	ON or OFF	ON or OFF

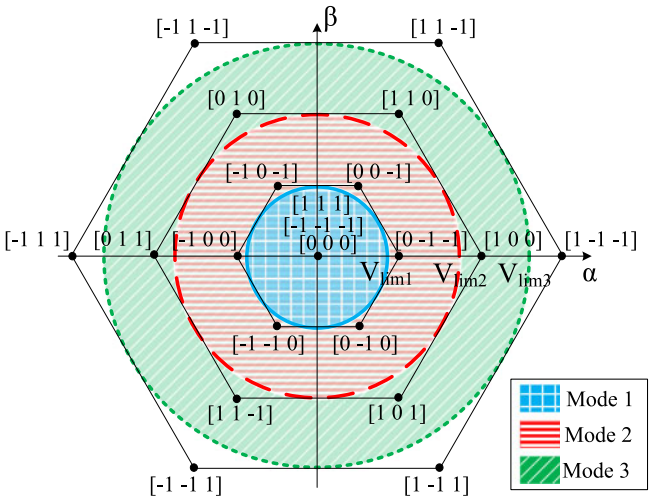

Fig. 5. Space representation in alpha-beta diagram of the adapted SVPWM.

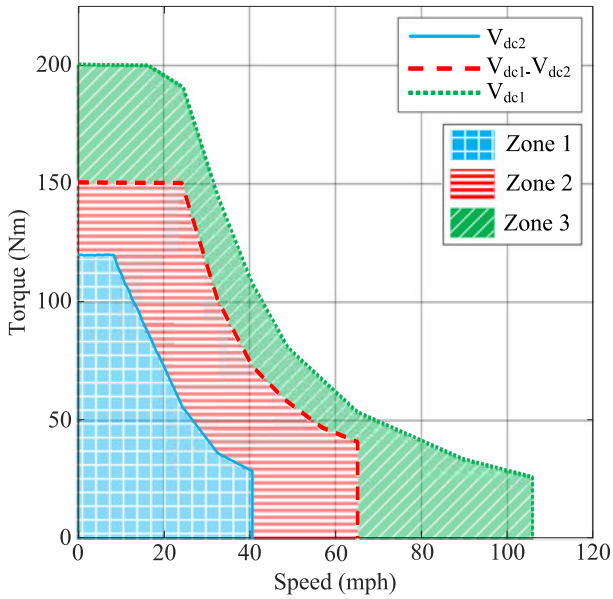

Fig. 6. Simplified torque-speed characteristic of the Toyota Prius from [5] combined with the operating modes of the multi-source inverter.

tors, such as the accelerations or braking. Moreover, the unique system configuration in power-split HEVs, such as the Toyota Prius, enables the power of the ICE to be shared between the electric machines and the differential of the vehicle. As a result, the power distribution can be controlled in order to optimize the efficiency of the ICE under several driving conditions [46].

A combination of the torque-speed characteristic of the Toyota Prius developed in [5] with the multi-source inverter's modes is presented in Fig. 6. The equivalent driving modes of the suggested hybrid powertrain with the multi-source inverter are shown in Fig. 7. The purpose of these simplified sketches is to illustrate the areas where the multi-source inverter's modes can be employed based on the control strategy applied in the Toyota Prius. In the low speed-low torque region shown by Zone 1 in Fig. 6, the vehicle operates in electric-only where the battery provides power to the wheels and the ICE is not used. Compared to conventional hybrid powertrains, the multi-source inverter can operate in Mode 1 and the battery supplies the motor without converting its voltage through the DC/DC boost converter [see Fig. 7(a)]. When the power required by the driver is too high to be provided by the battery alone, the ICE starts and the powertrain operates in either Zone 2 or 3 of Fig. 6, depending on the speed and torque requirements. In a conventional hybrid powertrain, two main control strategies are then achievable determined by the charge of the battery. If the battery does not need to be charged, the power from the ICE is split into two parts: one part goes directly to the differential of the vehicle to drive the wheels while the other part drives the electric machines. As a result, EM_1 operates as a generator and supplies the high DC-link current that drives EM_2 which supplements the ICE. This mode enables the ICE to operate at its ideal speed and torque level and, hence, ensures high efficiency and optimizes fuel economy. On the other hand, when the state-of-charge (SOC) of the battery is low, the power from EM_1 can be used to charge the battery while the ICE still meets the road requirements. Similarly to conventional hybrid powertrains, comparable control strategies can be applied to the suggested powertrain with the multi-source inverter. For middle speed and torque ranges delimited by Zone 2 in Fig. 6, the multi-source inverter can operates in Mode 2 and the battery can be charged by EM_1 with the additional benefit of not using the DC/DC converter as shown in Fig. 7(b). Moreover, when high speed and/or torque is required from the wheels, as in Zone 3, the multi-source can operate in Mode 3 where the battery is not used [see Fig. 7(c)]. Finally, it can be seen that the DC/DC converter will be only used to start the ICE and in regenerative braking [see Fig. 7(d)].

It should be noted that the above control strategies presented in Fig. 7 have been greatly simplified and require more analyses to be implemented. For instance, if the battery is fully charged or the maximum allowed charge current of the battery is lower than the resulting current, then the system shall exit Mode 2 and enter in Mode 3. In addition, if the SOC of the battery is low, the multi-source inverter should be forced to operate in Mode 2 in order to extend the charging opportunities. Nevertheless,

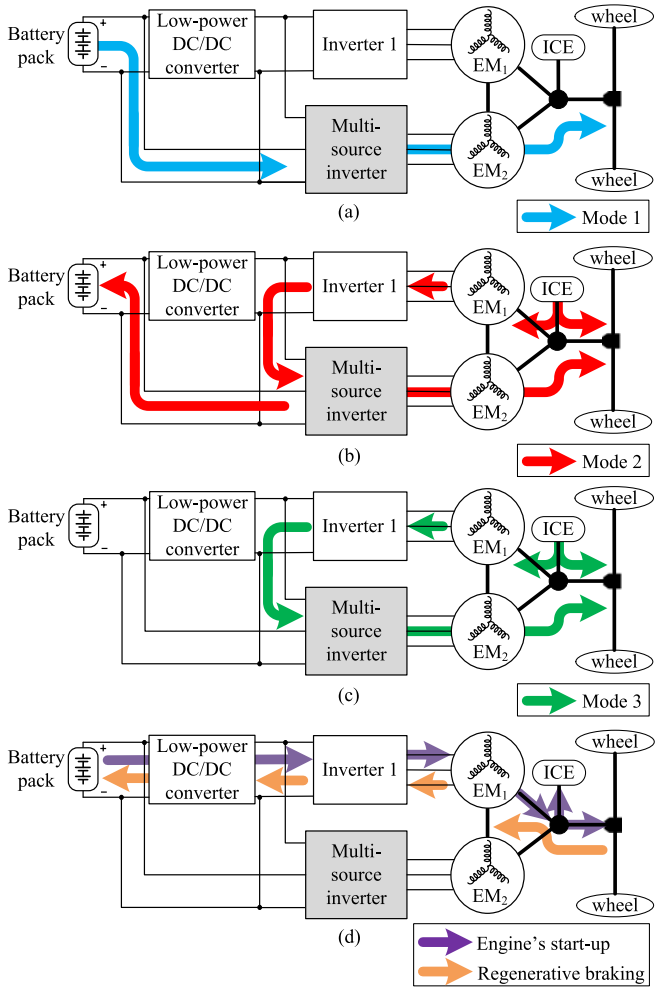

Fig. 7. Power flow in the driving modes of the proposed hybrid powertrain with the multi-source inverter in (a) Mode 1. (b) Mode 2. (c) Mode 3. (d) Engine′ s start-up and regenerative braking.

the DC/DC converter is never used in traction mode which not only impacts on the efficiency of the overall system but also enables reducing the power rating of this converter. Finally, one can notice that the charging opportunities of the battery are significantly extended since it can be achieved not only through regenerative braking such as in a conventional hybrid vehicle but also when the multi-source inverter operates in Mode 2. All these advantages could make the multi-source inverter a new option for the electrical propulsion system architecture in electrified vehicles.

IV. Simulation and Experimental Results

A dedicated speed control strategy using a conventional field oriented control (also called vector control) and the adapted SVPWM has been implemented and tested in simulations and experiments to validate the use of the multi-source inverter to drive an electric motor (see Fig. 8) [47]. Based on speed and current references, proportional integral (PI) controllers generate a reference voltage in alpha-beta axis whose module is compared to $V_{\mathrm{lim}1}$, $V_{\mathrm{lim}2}$, and $V_{\mathrm{lim}3}$ from Fig. 5 to determine the operating

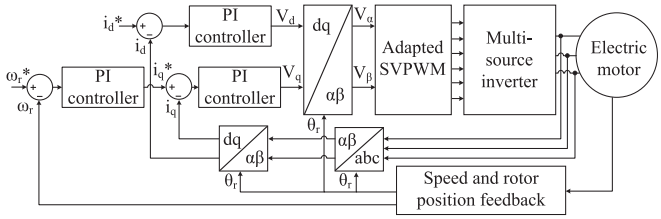

Fig. 8. New speed control scheme with the multi-source inverter.

TABLE III
Parameters of the Closed-Loop Control Model

Component	Parameter	Value
Input source voltages	V_{dc1}	150 V
	V_{dc2}	50 V
Multi-source inverter	Switching frequency	10 kHz
Induction motor	Power	10 HP
	Voltage	208 V to 230 V
	Current	27.6 A to 24.4 A
	Number of poles	2
	Stator resistance	0.135 Ω
	Rotor resistance	0.18 Ω
	Stator inductance	0.064 H
	Rotor inductance	0.064 H
	Inertia	0.1 $kg.m^2$
	Rated speed	3500 rpm

mode of the multi-source inverter. Then, the adapted SVPWM is applied to generate the gate signals as described in Section II-B.

A. Simulation Results

The closed-loop control model presented in Fig. 8 with an induction motor was developed in MATLAB/Simulink and parameters are listed in Table III. Input DC voltages were chosen in the same range as those used in the experiments. Simulations were performed with three different speed references (300 rpm, 700 rpm, and 1100 rpm), no torque and a constant reference current I_d^* of 13 A, showing the behavior of the multi-source inverter in each operating mode.

The simulation waveforms, presented in Figs. 9–11, are in line with the following theory:

- In Mode 1 (see Fig. 9), the battery supplies the motor whereas the high DC-link voltage is not being used, which is shown in the figure by a positive battery current while the high DC-link current remains null.
- In Mode 2 (see Fig. 10), a positive high DC-link current and a negative battery current are drawn, confirming the charge of the battery from the high DC-link voltage while the motor is running. One can also note that the battery current is equal to the negative of the high DC-link current (losses neglected). This is because in Mode 2 the two input sources are in series and the negative pole of the battery is connected to the negative pole of the high DC-link voltage. Hence, the current provided to drive the load is the same as the one charging the battery. This particular feature can adversely affect the battery lifetime since the

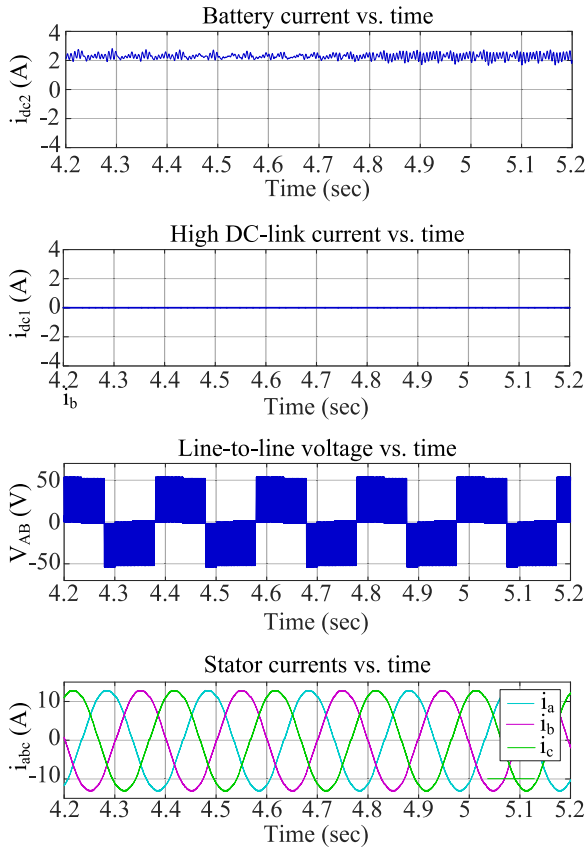

Fig. 9. Simulation results in Mode 1.

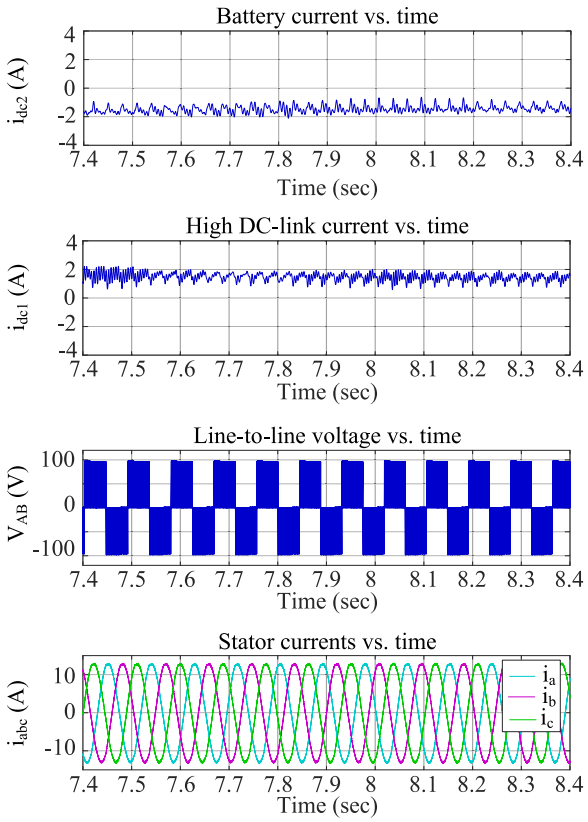

Fig. 10. Simulation results in Mode 2.

average value is not directly controllable and only depends on the current required by the load. A control strategy needs to be further investigated to avoid any inrush currents that could damage the battery.

- In Mode 3 (see Fig. 11), the battery current is null showing that the battery is not being used. In this mode the motor is driven by the high DC-link voltage, which is verified by a positive high DC-link current.

In Figs. 9–11, the line-to-line voltage V_{AB} varies according to the mode of the multi-source inverter as predicted by the theoretical analysis (see Table I). It can also be seen that the amplitudes of the stator currents i_a, i_b, and i_c are equal to I_d^*, which is due to the fact that in no load condition the current I_q is null. Moreover, their frequency increases as the rotor speed increases which is consistent with the theory.

B. Experimental Results

A scaled-down prototype was built to validate the effectiveness of the inverter and is composed of three IGBT modules type F3L50R06W1E3-B11 (see Fig. 12). Experiments were performed with the same closed-loop control model as presented in Fig. 8, a 5.9 kWh battery pack of 50 V and a high DC-link voltage of 150 V provided by a power supply (see Tables III and IV). In Fig. 13, it can be seen that an induction motor is connected back-to-back with an induction generator which can be used as a load by controlling the slip speed between the two machines.

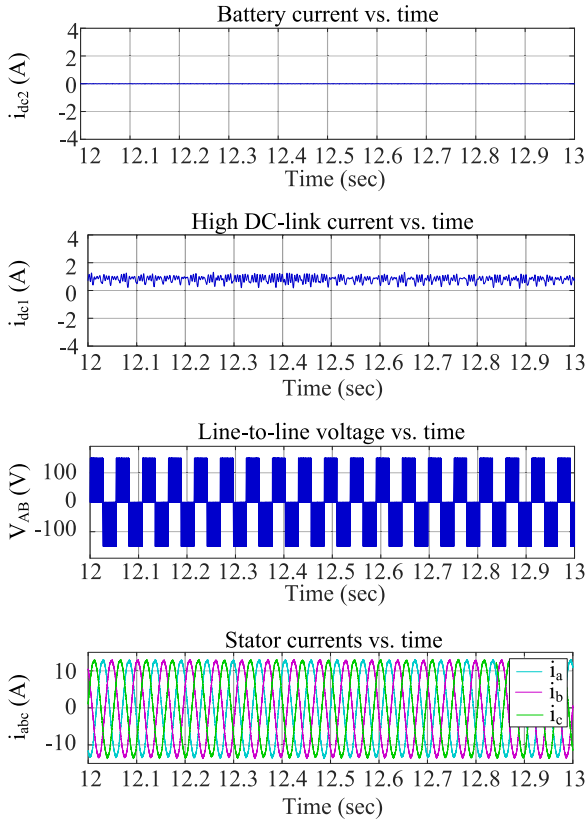

Fig. 11. Simulation results in Mode 3.

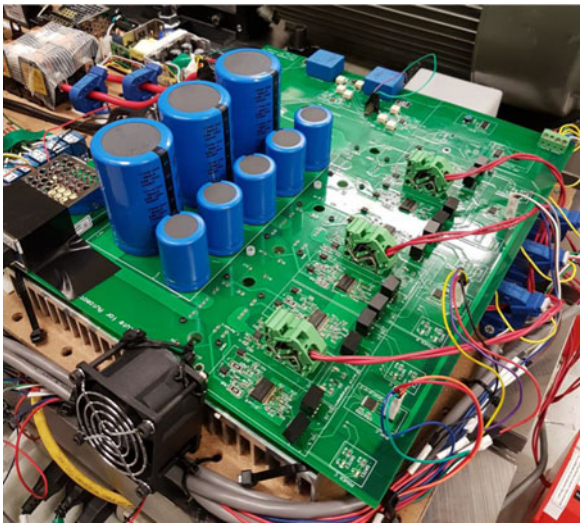

Fig. 12. Prototype of the multi-source inverter.

TABLE IV
PARAMETERS OF THE BATTERY PACK

Parameters	Value
Energy	5.9 kWh
Voltage (nominal)	50 V
Capacity	116 Ah

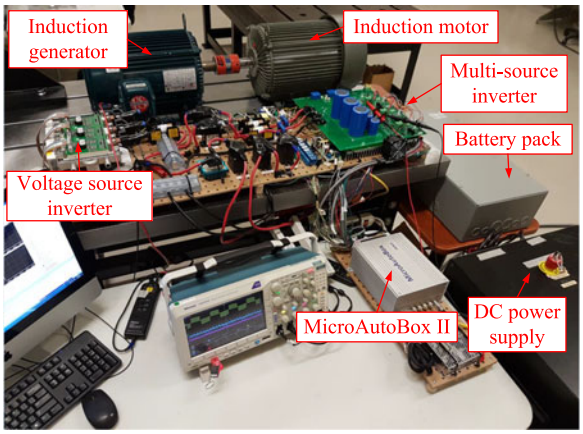

Fig. 13. Experimental test setup.

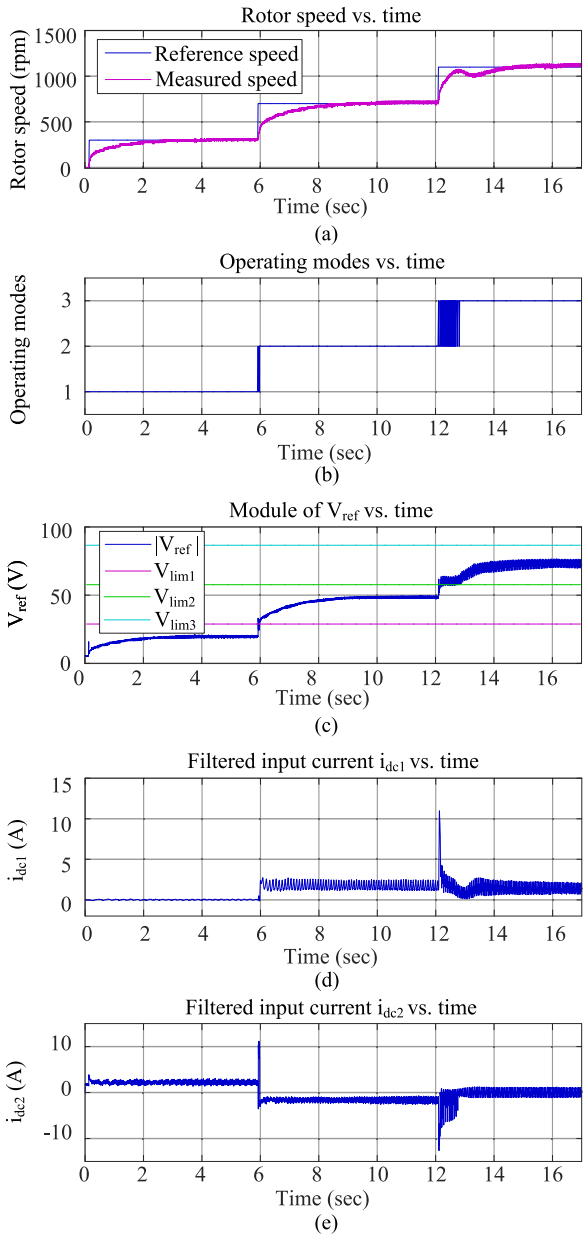

Fig. 14. Experimental results with (a) Rotor speed. (b) Operating modes. (c) Module of the reference voltage $|V_{\rm ref}|$. (d) Filtered input DC current $i_{\rm dc1}$. (e) Filtered input DC current $i_{\rm dc2}$.

However, in the following results no torque has been applied. The control of the overall setup including the gate signals of the multi-source inverter as well as the measured currents, voltages, and speed are managed by a real-time system MicroAutoBox II and the software dSPACE. Experiments have been carried out with three different speeds (300 rpm, 700 rpm, and 1100 rpm), no torque and a constant reference current I_d^* of 13 A. Results are presented from Figs. 14 to 17.

As shown in Fig. 14(a), the rotor speed converges to the three different reference values and it can be seen in Fig. 14(b) that the multi-source inverter switches between the operating modes as expected. Indeed, when the module of reference voltage $|V_{\rm ref}|$ is lower than $V_{\rm lim,1}$, the multi-source inverter operates in Mode 1; if $|V_{\rm ref}|$ stays between $V_{\rm lim,1}$ and $V_{\rm lim,2}$ the multi-source inverter is in Mode 2 and finally if $|V_{\rm ref}|$ is between $V_{\rm lim,2}$ and $V_{\rm lim,3}$, the multi-source inverter operates in Mode 3 [see Fig. 14(c)]. Fig. 14(d) and (e) show the filtered input DC currents $i_{\rm dc1}$ and $i_{\rm dc2}$ for the three operating modes. In Mode 1, the battery current is positive while the high DC-link current $i_{\rm dc1}$ is almost null. These results confirm the theory where in Mode 1 only the battery supplies the load. In Mode 2, the battery current is negative and equal to the inverse of the current $i_{\rm dc1}$, which validates that the high DC-link voltage supplies power to the induction motor and charges the battery at the same time. In Mode 3, it can be seen that the battery current is almost equal to zero ampere, allowing considering the battery as OFF. One can

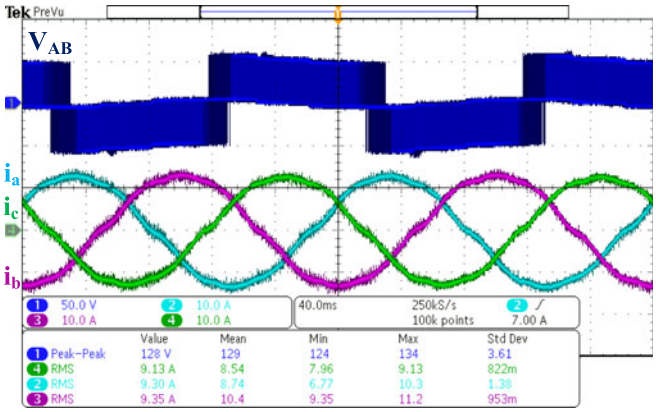

Fig. 15. Experimental waveforms in Mode 1 with the voltage V_{AB} and the stator currents i_a, i_b and i_c.

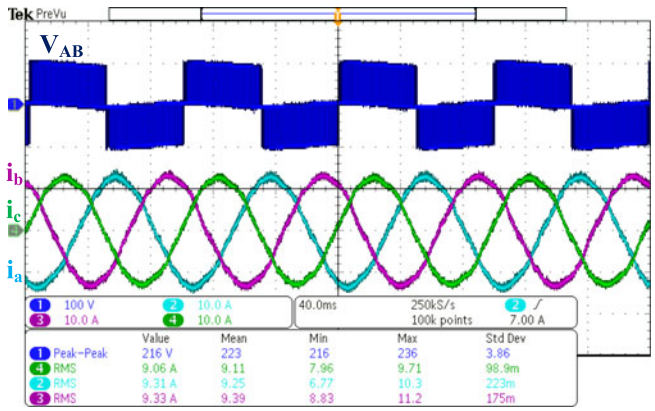

Fig. 16. Experimental waveforms in Mode 2 with the voltage V_{AB} and the stator currents i_a, i_b and i_c.

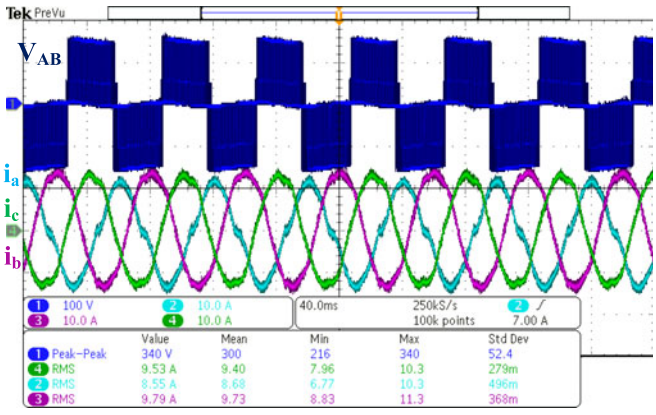

Fig. 17. Experimental waveforms in Mode 3 with the voltage V_{AB} and the stator currents i_a, i_b, and i_c.

also note that in Mode 3 the input DC currents are noisier than in the other modes, this is due to the imbalance of the induction motor which becomes more noticeable at high speed.

In Figs. 15–17, the line-to-line voltage V_{AB} and the three-phase stator currents i_a, i_b, and i_c in Modes 1, 2, and 3 respectively are shown. The peak-to-peak value of V_{AB} in each mode is comparable to the theoretical values from Table I and the small discrepancies can be explained by the voltage across the phase impedance Z_i that was neglected in the table. Moreover, one can note that the amplitudes of the stator currents i_a, i_b, and i_c are equal to the reference current I_d^* since no torque and, hence, a current I_q equal to zero has been applied. Finally the imbalance of the induction motor mentioned in the previous paragraph can be noticed in Fig. 17 at high speed where the rms value of i_a has more than 1A difference compared to i_b and i_c while it was not the case in Mode 1 and 2.

According to the theoretical principle of operation and simulations, the experimental results are consistent. Moreover, each mode commutes well according to the rotor speed reference requested.

V. Conclusion

In this paper, an inverter topology suitable for HEVs and PHEVs was proposed. The multi-source inverter allows independent DC sources to drive the propulsion motor while directly using the battery voltage as one of the voltage levels. As a result, this power inverter enables an adaptable voltage to supply the motor without the use of a DC/DC boost converter. Then, this DC/DC converter is not used in traction mode and will only help starting the ICE and in regenerative braking. By doing so, the overall efficiency of the hybrid powertrain can be improved and the power rating of the DC/DC converter can be significantly reduced. Another advantage of the topology is the extension of the charging opportunities of the battery while the motor is running. However, one can note that a charging current control needs to be further investigated to prevent the battery from hazardous inrush currents. Simulation and experiments have been performed in closed-loop control with an induction motor to verify and validate the theoretical principle of operation of the suggested inverter. In view of the promising results, the multi-source inverter could offer a new option for the electrical propulsion system architecture in electrified vehicles.

References

[1] B. Bilgin *et al.*, "Making the case for electrified transportation," *IEEE Trans. Transp. Electrification*, vol. 1, no. 7, pp. 4–17, Jun. 2015.
[2] C. C. Chan, "The state of the art of electric, hybrid, and fuel cell vehicles," *Proc. IEEE*, vol. 95, no. 4, pp. 704–718, Apr. 2007.
[3] C. Ma, M. Song, J. Ji, J. Park, S. Ko, and H. Kim, "Comparative study on power characteristics and control strategies for plug-in HEV," in *Proc. 2011 IEEE Veh. Power Propulsion Conf.*, Chicago, IL, USA, Sep. 2011, pp. 1–6.
[4] A. Emadi, *Advanced Electric Drive Vehicles*. Boca Raton, FL, USA: CRC Press, Oct. 2014.
[5] T. A. Burress *et al.*, "Evaluation of the 2010 Toyota Prius hybrid synergy drive system," Oak Ridge Nat. Lab., Oak Ridge, TN, USA, Tech. Rep. ORNL/TM-2010/253, Jan. 2008.
[6] I. N. L. (INL). Advanced Vehicles - Vehicle Testing. [Online]. Available: https://avt.inl.gov/vehicle-type/all-powertrain-architecture
[7] A. Emadi, S. S. Williamson, and A. Khaligh, "Power electronics intensive solutions for advanced electric, hybrid electric, and fuel cell vehicular power systems," *IEEE Trans. Power Electron.*, vol. 21, no. 3, pp. 567–577, May 2006.
[8] J. M. Miller, "Power electronics in hybrid electric vehicle applications," in *Proc. 2003 18th Annu. IEEE Appl. Power Electron. Conf. Expo.*, Miami Beach, FL, USA, Feb. 2003, pp. 23–29.
[9] U. S. Drive, "Electrical and electronics technical team roadmap," *Partnership Plan, Roadmaps, and Other Documents*, Jun. 2013.
[10] B. Ozpineci. Power electronics and thermal management breakout session. Jul. 2012, [Online]. Available: http://www.energy.gov/

[11] S. Rogers. Electric drive status and challenges. Jul. 2012, [Online]. Available: http://www.energy.gov/
[12] T. Burress and S. Campbell, "Benchmarking EV and HEV power electronics and electric machines," in *Proc. 2013 IEEE Transp. Electrification Conf. Expo*, Metro Detroit, MI, USA, Jun. 2013, pp. 1–6.
[13] R. Staunton, T. A. Burress, and L. D. Marlino, "Evaluation of the 2005 Honda Accord hybrid synergy drive system," Oak Ridge Nat. Lab., Oak Ridge, TN, USA, Tech. Rep. ORNL/TM-2006/535, Sep. 2006.
[14] T. A. Burress *et al.*, "Evaluation of the 2008 Lexus LS 600H hybrid synergy drive system," Oak Ridge Nat. Lab., Oak Ridge, TN, USA, Tech. Rep. ORNL/TM-2008/185, Jan. 2009.
[15] T. A. Burress *et al.*, "Evaluation of the 2007 Toyota Camry hybrid synergy drive system," Oak Ridge Nat. Lab., Oak Ridge, TN, USA, Tech. Rep. ORNL/TM-2007/190, May 2011.
[16] T. Burress, "Benchmarking EV and HEV technologies," in *Proc. U.S. DOE Veh. Technol. Office 2015 Annu. Merit Rev. Peer Eval. Meeting*, Jun. 2016, pp. 254–266.
[17] J. O. Estima and A. J. M. Cardoso, "Efficiency analysis of drive train topologies applied to electric/hybrid vehicles," *IEEE Trans. Veh. Technol.*, vol. 61, no. 3, pp. 1021–1031, Mar. 2012.
[18] K. Asano, Y. Inaguma, H. Ohtani, E. Sato, M. Okamura, and S. Sasaki, "High performance motor drive technologies for hybrid vehicles," in *Proc. 2007 IEEE Power Convers. Conf.*, Nagoya, Japan, Apr. 2007, pp. 1584–1589.
[19] M. Olszewski, "Boost converters for gas electric and fuel cell hybrid electric vehicles," Oak Ridge Nat. Lab., Oak Ridge, TN, USA, Tech. Rep. ORNL/TM-2005/53, Jun. 2005.
[20] H. Ye, P. Magne, B. Bilgin, S. Wirasingha, and A. Emadi, "A comprehensive evaluation of bidirectional boost converter topologies for electrified vehicle applications," in *Proc. IECON 2014-40th Annu. Conf. IEEE Ind. Electron. Soc.*, Dallas, TX, USA Oct. 2014, pp. 2914–2920.
[21] B. A. Welchko and J. M. Nagashima, "The influence of topology selection on the design of EV/HEV propulsion systems," *IEEE Power Electron. Lett.*, vol. 1, no. 2, pp. 36–40, Jun. 2003.
[22] I. Staudt, "3L NPC and TNPC topology," SEMIKRON, Nuremberg, Germany, Tech. Rep. AN-11001, Oct. 2012.
[23] M. Schweizer and J. W. Kolar, "Design and implementation of a highly efficient three-level T-type converter for low-voltage applications," *IEEE Trans. Power Electron.*, vol. 28, no. 2, pp. 899–907, Feb. 2013.
[24] J. Rodriguez, S. Bernet, P. K. Steimer, and I. E. Lizama, "A survey on neutral-point-clamped inverters," *IEEE Trans. Ind. Electron.*, vol. 57, no. 7, pp. 2219–2230, Jul. 2010.
[25] R. Teichmann and S. Bernet, "A comparison of three-level converters versus two-level converters for low-voltage drives, traction, and utility applications," *IEEE Trans. Ind. Appl.*, vol. 41, no. 3, pp. 855–865, May/Jun. 2005.
[26] M. Schweizer, I. Lizama, T. Friedli, and J. W. Kolar, "Comparison of the chip area usage of 2-level and 3-level voltage source converter topologies," in *Proc. IECON 2010-36th Annu. Conf. IEEE Ind. Electron. Soc.*, Glendale, AZ, USA, Nov. 2010, pp. 391–396.
[27] P. C. Loh, F. Gao, and F. Blaabjerg, "Topological and modulation design of three-level Z-source inverters," *IEEE Trans. Power Electron.*, vol. 23, no. 5, pp. 2268–2277, Nov. 2008.
[28] S. Bhattacharya, D. Mascarella, G. Joós, J.-M. Cyr, and J. Xu, "A dual three-level T-NPC inverter for high-power traction applications," *IEEE J. Emerg. Select. Topics Power Electron.*, vol. 4, no. 2, pp. 668–678, Jun. 2016.
[29] G. Mondal, K. Sivakumar, R. Ramchand, K. Gopakumar, and E. Levi, "A dual seven-level inverter supply for an open-end winding induction motor drive," *IEEE Trans. Ind. Electron.*, vol. 56, no. 5, pp. 1665–1673, May 2009.
[30] A. Battiston, J.-P. Martin, E.-H. Miliani, B. Nahid-Mobarakeh, S. Pierfederici, and F. Meibody-Tabar, "Comparison criteria for electric traction system using z-source/quasi z-source inverter and conventional architectures," *IEEE J. Emerg. Select. Topics Power Electron.*, vol. 2, no. 3, pp. 467–476, Sep. 2014.
[31] O. Hegazy, J. Van Mierlo, and P. Lataire, "Design and control of bidirectional DC/AC and DC/DC converters for plug-in hybrid electric vehicles," in *Proc. 2011 Int. Conf. Power Eng., Energy Electr. Drives*, Malaga, Spain, May 2011, pp. 1–7.
[32] M. Wang and K. Tian, "A nine-switch three-level inverter for electric vehicle applications," in *Proc. 2008 IEEE Veh. Power Propulsion Conf.*, Harbin, Hei Longjiang, China, Sep. 2008, pp. 1–5.
[33] V. F. Pires, A. Cordeiro, D. Foito, and J. F. Martins, "Quasi-Z-source inverter with a T-type converter in normal and failure Mode," *IEEE Trans. Power Electron.*, vol. 31, no. 11, pp. 7462–7470, Jan. 2016.
[34] F. Z. Peng, M. Shen, and K. Holland, "Application of Z-source inverter for traction drive of fuel cellbattery hybrid electric vehicles," *IEEE Trans. Power Electron.*, vol. 22, no. 3, pp. 1054–1061, May 2007.
[35] H. Ye, Y. Yang, and A. Emadi, "Traction inverters in hybrid electric vehicles," in *Proc. 2012 IEEE Transp. Electrification Conf. Expo*, Dearborn, MI, USA, Jun. 2012, pp. 1–6.
[36] M. Shen, A. Joseph, J. Wang, F. Z. Peng, and D. J. Adams, "Comparison of traditional inverters and Z-source inverter for fuel cell vehicles," *IEEE Trans. Power Electron.*, vol. 22, no. 4, pp. 1453–1463, Jul. 2007.
[37] A. Emadi and P. Magne, "Power Converter," Patent U.S. 0 117 770 A1, May 1, 2014.
[38] L. Dorn-Gomba, P. Magne, C. Barthelmebs, and A. Emadi, "On the concept of the multi-source inverter," in *Proc. 2016 IEEE Appl. Power Electron. Conf. Expo.*, Long Beach, CA, USA, Mar. 2016, pp. 453–459.
[39] S. P. Singh and R. K. Tripathi, "Performance comparison of SPWM and SVPWM technique in NPC bidirectional converter," in *Proc. 2013 Students Conf. Eng. Syst.*, Allahabad, India, Apr. 2013, pp. 1–6.
[40] X. Jing, J. He, and N. A. O. Demerdash, "Loss balancing SVPWM for active NPC converters," in *Proc. 2014 29th Annu. IEEE Appl. Power Electron. Conf. Expo.*, Fort Worth, TX, USA, Mar. 2014, pp. 281–288.
[41] K. V. Kumar, P. A. Michael, J. J. P., and S. K. S., "Simulation and comparison of SPWM and SVPWM control for three phase inverter," *ARPN J. Eng. Appl. Sci.*, vol. 5, no. 7, pp. 61–74, Jul. 2010.
[42] V. Xue, "Center-aligned SVPWM realization for 3-phase 3-level inverter," Texas Instrument, Dallas, TX, USA, Tech. Rep. SPRABS6, Oct. 2012.
[43] K. Ç. Bayindir, M. A. Gözüküçük, and A. Teke, "A comprehensive overview of hybrid electric vehicle: Powertrain configurations, powertrain control techniques and electronic control units," *Energy Convers. Manage.*, vol. 52, no. 2, pp. 1305–1313, 2011.
[44] M. Ehsani, Y. Gao, and A. Emadi, *Modern Electric, Hybrid Electric, and Fuel Cell Vehicles: Fundamentals, Theory, and Design*. Boca Raton, FL, USA: CRC press, 2009.
[45] E. Rask *et al.*, "Model year 2010 (Gen 3) Toyota Prius level 1 testing report," Argonne Nat. Lab., Lemont, IL, USA, Tech. Rep. ANL/ES/RP-67317, Jul. 2010.
[46] M. Zhang, P. Suntharalingam, Y. Yang, and W. Jiang, "Fundamentals of hybrid electric powertrains," in *Advanced Electric Drive Vehicles*. Lemont, IL, USA: CRC Press p, Oct. 2014, ch. 11, pp. 369–389.
[47] D. Y. Ohm, *Dynamic Model of Induction Motors for Vector Control.* Blacksburg, VA, USA: Drivetech, Inc., 2001, pp. 1–10.

Lea Dorn-Gomba (S'15) received the M.Eng. degree in electrical engineering from Ecole Nationale Supérieure d'Électricité et de Mécanique, Nancy, France, in 2014. She is currently working toward the Ph.D. degree in electrical engineering at the Canada Excellence Research Chair in Hybrid Powertrain Program, McMaster University, Hamilton, ON, Canada,

In 2015, she joined the McMaster Automotive Resource Centre at McMaster University. Her research interests include power electronics design and control and electrified vehicle powertrains.

Pierre Magne (S'11–M'13) received the M.Sc. degree in electrical and electronics engineering from the Institut National Polytechnique de Lorraine, Nancy, France, in 2009, and the M.Eng. degree in electrical engineering from the Ecole Nationale Supérieure d'Électricité et de Mécanique, Nancy, France, in 2009. He received the Ph.D. degree in electrical engineering from the University of Lorraine, Nancy, France, in 2012.

He is currently working as a Technical Manager in APOJEE, Clermont-Ferrand, France. Prior to that, he holds Engineering positions in Schneider Electric and was a Principal Research Engineer for the Canada Excellence Research Chair in Hybrid Powertrain Program, McMaster University. His current research interests include power electronics, powertrain technologies, and nonlinear controls and their applications.

Benjamin Danen received the Bachelor of Engineering and Masters of Engineering degrees in electrical engineering from McMaster University, Hamilton, ON, Canada, in 2014 and 2016, respectively.

In September 2014, he joined MARC as a Research Assistant for the Canada Excellence Research Chair in Hybrid Powertrain Program where he currently serves as a Research Engineer. His research interests include motor control, system modeling, and power electronics.

Ali Emadi (S'98–M'00–SM'03–F'13) received the B.S. and M.S. degrees in electrical engineering with highest distinction from Sharif University of Technology, Tehran, Iran, in 1995 and 1997, respectively, and the Ph.D. degree in electrical engineering from Texas A&M University, College Station, TX, USA, in 2000.

He is the Canada Excellence Research Chair in Hybrid Powertrain at McMaster University in Hamilton, ON, Canada. Before joining McMaster University, he was the Harris Perlstein Endowed Chair Professor of Engineering and the Director of the Electric Power and Power Electronics Center and Grainger Laboratories at Illinois Institute of Technology, Chicago, IL, USA, where he established research and teaching facilities as well as courses in power electronics, motor drives, and vehicular power systems. He was the Founder, Chairman, and President of Hybrid Electric Vehicle Technologies, Inc. a university spin-off company of Illinois Tech.

Dr. Emadi received the numerous awards and recognitions. He was the advisor for the Formula Hybrid Teams at Illinois Tech and McMaster University, which won the GM Best Engineered Hybrid System Award in 2010, 2013, and 2015 competitions. He is the Principal author/coauthor more than 400 journal and conference papers as well as several books including Vehicular Electric Power Systems (2003), Energy Efficient Electric Motors (2004), Uninterruptible Power Supplies and Active Filters (2004), Modern Electric, Hybrid Electric, and Fuel Cell Vehicles (2nd ed, 2009), and Integrated Power Electronic Converters and Digital Control (2009). He is also the Editor of the Handbook of Automotive Power Electronics and Motor Drives (2005) and Advanced Electric Drive Vehicles (2014). He was the Inaugural General Chair of the 2012 IEEE Transportation Electrification Conference and Expo and has chaired several IEEE and SAE conferences in the areas of vehicle power and propulsion. He is the founding Editor-in-Chief of the IEEE TRANSACTIONS ON TRANSPORTATION ELECTRIFICATION.